ACTA SCIENTIAE

ISSN: 2178-7727

Application Of Core-Shell Nanoparticles of CuI/Ag,Cu AND CuS/Ag,Cu For Diverse Optical Properties

Varun Kumar[1], Surbhi[2], Santosh Madhav Walke[3]

[1]Amity Institute of Applied Sciences, AMITY University, Noida UP, India

[2]Amity Institute of Applied Sciences, AMITY University, Noida UP, India.

[3]C-311, Maruti Niwas, Plot No. B-37, Sector 06, New Panvel East, Navi Mumbai – 410206
Near Phadke Highschool, Maharashtra

ABSTRACT

Core-shell nanoparticles have emerged as promising materials for optical applications due to their tunable properties and enhanced stability. This research investigates the synthesis, characterization, and optical properties of copper iodide and copper sulfide-based core-shell nanoparticles with silver and copper shells. We synthesized CuI/Ag,Cu and CuS/Ag,Cu nanoparticles using chemical reduction methods and characterized them using UV-Visible spectroscopy, X-ray diffraction, and transmission electron microscopy. The optical absorption spectra revealed distinct surface plasmon resonance peaks, with CuI/Ag,Cu nanoparticles showing absorption maxima at 420 nm and CuS/Ag,Cu at 385 nm. Particle size analysis indicated average diameters of 25-35 nm for CuI-based structures and 18-28 nm for CuS-based structures. The core-shell architecture demonstrated superior optical stability compared to single-component nanoparticles, with enhanced photoluminescence properties. Our findings suggest that these nanoparticles hold significant potential for applications in photocatalysis, sensing devices, and optoelectronic systems. The research contributes to understanding how core-shell composition influences optical behavior and provides practical synthesis protocols for developing advanced nanomaterials with tailored properties.

KEYWORDS: Core-shell nanoparticles, Copper iodide, Copper sulfide, Silver, Surface plasmon resonance, Optical properties, Nanomaterials

INTRODUCTION

Nanotechnology has revolutionized materials science by enabling the manipulation of matter at atomic and molecular scales. Among various nanostructures, core-shell nanoparticles have attracted considerable attention because they combine properties of different materials in a single entity. The core provides structural foundation while the shell offers protection and additional functionality. This architectural design creates opportunities for applications that single-component nanoparticles cannot achieve effectively.

Metal and semiconductor nanoparticles exhibit unique optical properties due to quantum confinement effects and surface plasmon resonance phenomena. When light interacts with these materials at the nanoscale, electrons oscillate collectively, creating strong absorption and scattering effects. Researchers have extensively studied gold and silver nanoparticles for their excellent plasmonic properties, but cost and availability issues motivate exploration of alternative materials (Zhang and Wang, 2023).

Copper-based nanoparticles present economically viable alternatives with interesting optical characteristics. Copper iodide is a p-type semiconductor with a direct bandgap of approximately 3.1 eV, making it transparent in the visible spectrum while exhibiting photoconductivity. Copper sulfide exists in multiple stoichiometric phases, each displaying different optical and electronic properties. The ability to control these phases offers additional tuning mechanisms for material design (Kumar et al., 2022).

However, copper nanoparticles suffer from oxidation instability when exposed to ambient conditions. This degradation severely limits their practical applications. Creating protective shells around copper cores addresses this challenge while introducing new functionalities. Silver and copper shells provide both protection and enhanced optical properties through synergistic effects between core and shell materials.

DOI: 10.22178/acta.26.1.30

ISSN: 2178-7727

Previous research has demonstrated core-shell structures using various material combinations. Studies on Au/Ag nanoparticles showed how shell thickness affects plasmon resonance wavelengths (Martinez and Chen, 2023). Research on semiconductor cores with metallic shells revealed enhanced photocatalytic activity due to improved charge separation. Yet comprehensive investigations of CuI and CuS cores with bimetallic Ag,Cu shells remain limited in the literature.

This research addresses several critical questions. How do CuI/Ag,Cu and CuS/Ag,Cu core-shell nanoparticles differ in their optical absorption characteristics? What particle sizes and distributions result from our synthesis approach? How does the core-shell architecture influence photoluminescence behavior? Can we establish relationships between structural features and optical performance?

The significance of this work extends beyond fundamental science. Developing cost-effective nanoparticles with tunable optical properties enables advances in solar energy conversion, environmental remediation through photocatalysis, biological sensing, and display technologies. Understanding structure-property relationships in these systems provides design principles for engineering nanomaterials with specific characteristics.

Our study synthesizes both types of core-shell nanoparticles using chemical methods, thoroughly characterizes their structural and optical properties, and compares their performance. The research reveals how core composition influences the resulting optical behavior and demonstrates the advantages of core-shell architectures over simple nanoparticles.

OBJECTIVES

The research pursues the following objectives:

- **Primary Objective:** Synthesize and characterize CuI/Ag,Cu and CuS/Ag,Cu core-shell nanoparticles to investigate their distinct optical properties and establish structure-property relationships.
- **Objective 1:** Develop reproducible synthesis protocols for producing uniform core-shell nanoparticles with controlled size distributions.
- **Objective 2:** Characterize the structural properties of synthesized nanoparticles using X-ray diffraction and transmission electron microscopy to confirm core-shell formation.
- **Objective 3:** Analyze the optical absorption and photoluminescence properties of both nanoparticle types to identify key differences arising from core composition.
- **Objective 4:** Compare the optical stability of core-shell nanoparticles against single-component nanoparticles to demonstrate the protective benefits of shell layers.

SCOPE OF STUDY

This research encompasses:

- **Material Scope:** Investigation focuses on CuI/Ag,Cu and CuS/Ag,Cu core-shell nanoparticles synthesized through wet chemical methods, excluding other copper compounds or shell compositions.
- **Characterization Scope:** Structural analysis via XRD and TEM, optical characterization through UV-Vis spectroscopy and photoluminescence measurements, with particle size distribution analysis.
- **Application Scope:** Discussion emphasizes optical applications including photocatalysis and sensing rather than electrical or magnetic properties.
- **Synthesis Scope:** Room temperature chemical reduction synthesis in aqueous media, excluding high-temperature methods, vapor deposition, or organic solvent systems.
- **Exclusions:** The study does not investigate biological toxicity, large-scale production economics, or device fabrication beyond proof-of-concept demonstrations.

LITERATURE REVIEW

4.1 Core-Shell Nanoparticle Fundamentals

Core-shell nanoparticles represent an advanced class of composite nanomaterials where one material forms

DOI: 10.22178/acta.26.1.30

ISSN: 2178-7727

the core and another creates a surrounding shell. This architecture provides several advantages over homogeneous nanoparticles. The shell protects chemically reactive cores from environmental degradation, preventing oxidation and aggregation. Core-shell structures also enable property tuning by varying core size, shell thickness, or material composition (Rahman et al., 2023).

The synthesis of core-shell nanoparticles typically involves two-stage processes. First, core nanoparticles are prepared through nucleation and growth. Subsequently, shell precursors deposit onto core surfaces through heterogeneous nucleation. Controlling these processes determines the final particle architecture, including shell completeness and uniformity. Various synthesis methods exist, including chemical reduction, sol-gel processes, and electrochemical deposition, each offering different advantages for specific material combinations.

4.2 Optical Properties of Metal Nanoparticles

Metal nanoparticles exhibit surface plasmon resonance, a phenomenon where conduction electrons oscillate collectively in response to electromagnetic radiation. This resonance creates strong absorption and scattering at specific wavelengths determined by particle size, shape, and surrounding medium. For silver nanoparticles, plasmon resonance typically occurs between 380-450 nm in aqueous solutions (Li and Thompson, 2024).

Copper nanoparticles also display plasmonic behavior, though less prominently than gold or silver due to interband transitions that dampen plasmon oscillations. The plasmon peak for copper nanoparticles appears around 560-600 nm. However, copper oxidizes readily in air, forming Cu_2O or CuO layers that significantly alter optical properties. This instability has limited copper's use in plasmonic applications despite its abundance and low cost.

4.3 Copper Iodide Semiconductor Properties

Copper iodide exists primarily in the γ-phase at room temperature, exhibiting a zinc blende crystal structure. As a p-type semiconductor with a wide bandgap, CuI shows transparency in the visible region while absorbing strongly in the ultraviolet. The material demonstrates high hole mobility and has found applications in transparent electronics and photovoltaics (Singh and Patel, 2023).

At the nanoscale, CuI exhibits quantum confinement effects when particle dimensions approach the exciton Bohr radius. This confinement increases the effective bandgap and creates discrete energy levels, leading to size-dependent optical properties. Nanocrystalline CuI also displays photoluminescence with emission wavelengths depending on particle size and surface conditions.

4.4 Copper Sulfide Phases and Properties

Copper sulfide exists in numerous stoichiometric and non-stoichiometric phases, including Cu_2S, $Cu_{1.8}S$, CuS, and intermediate compositions. These phases exhibit different crystal structures and electronic properties ranging from semiconducting to metallic behavior. Covellite (CuS) is particularly interesting for optical applications due to its narrow bandgap around 2.0 eV and strong near-infrared absorption (Anderson et al., 2022).

The ability to control copper sulfide phase during synthesis enables tuning of optical and electronic properties. Research has shown that particle size, synthesis temperature, and sulfur-to-copper ratio all influence the final phase composition. Copper sulfide nanoparticles have demonstrated promise in photothermal therapy, photocatalysis, and solar energy conversion due to their strong light absorption characteristics.

4.5 Bimetallic Shell Systems

Bimetallic shells composed of two metals offer advantages over single-metal shells by combining beneficial properties of both components. Silver provides excellent plasmonic properties and antimicrobial activity, while copper contributes to catalytic activity and reduces material costs. The interaction between silver and

DOI: 10.22178/acta.26.1.30

ISSN: 2178-7727

copper in alloy or layered shells can create synergistic effects enhancing overall performance (Wilson and Garcia, 2023).

Previous studies on Ag-Cu bimetallic nanoparticles revealed interesting optical behavior. Alloying silver with copper shifts the plasmon resonance compared to pure silver, with the exact wavelength depending on composition ratio. The bimetallic structure also improves stability compared to pure copper nanoparticles by reducing oxidation susceptibility.

4.6 Research Gaps

While extensive research exists on noble metal core-shell nanoparticles, systematic studies of copper halide and chalcogenide cores with bimetallic shells remain limited. Specifically, comparative investigations of how different core materials influence optical properties when combined with similar shell compositions are scarce. Most existing studies focus on single core-shell combinations rather than systematic comparisons that reveal structure-property relationships.

Additionally, practical synthesis protocols for CuI and CuS-based core-shell nanoparticles suitable for optical applications need further development. Many reported methods require complex equipment, high temperatures, or toxic reagents that limit accessibility. Simple, reproducible approaches would accelerate research and application development in this area.

RESEARCH METHODOLOGY

5.1 Materials and Chemicals

All chemicals were analytical grade and used without further purification. Copper sulfate pentahydrate ($CuSO_4 \cdot 5H_2O$) served as the copper source. Silver nitrate ($AgNO_3$) provided silver ions for shell formation. Potassium iodide (KI) supplied iodide for CuI synthesis. Sodium sulfide (Na_2S) acted as the sulfur source for CuS preparation. Sodium borohydride ($NaBH_4$) functioned as the reducing agent. Polyvinylpyrrolidone (PVP) served as a stabilizing agent to prevent aggregation. Deionized water was used as the solvent throughout all syntheses.

5.2 Synthesis of CuI/Ag,Cu Core-Shell Nanoparticles

Core synthesis began by dissolving 0.5 g $CuSO_4 \cdot 5H_2O$ in 50 mL deionized water under magnetic stirring. A solution of 0.8 g KI in 20 mL water was added dropwise to the copper solution, immediately forming a white precipitate of CuI. The mixture stirred for 30 minutes to ensure complete reaction. PVP (0.5 g) was then added to stabilize the nanoparticles.

For shell formation, a solution containing $AgNO_3$ (0.1 g) and $CuSO_4 \cdot 5H_2O$ (0.05 g) in 30 mL water was prepared separately. This bimetallic precursor solution was added slowly to the CuI suspension under vigorous stirring. Subsequently, $NaBH_4$ solution (0.2 g in 10 mL water) was introduced dropwise to reduce the metal ions onto the CuI core surfaces. The reaction proceeded for 2 hours at room temperature. The resulting nanoparticles were collected by centrifugation at 8000 rpm for 15 minutes, washed three times with deionized water, and dried at 60°C.

5.3 Synthesis of CuS/Ag,Cu Core-Shell Nanoparticles

CuS cores were synthesized by dissolving 0.5 g $CuSO_4 \cdot 5H_2O$ in 50 mL deionized water. A solution of 0.4 g Na_2S in 20 mL water was prepared and added dropwise to the copper solution, forming a black CuS precipitate. The mixture stirred for 45 minutes, followed by addition of 0.5 g PVP for stabilization.

The shell deposition process followed the same procedure as for CuI cores. A bimetallic precursor solution of $AgNO_3$ (0.1 g) and $CuSO_4 \cdot 5H_2O$ (0.05 g) in 30 mL water was added to the CuS suspension. $NaBH_4$ solution (0.2 g in 10 mL water) was then introduced to reduce metal ions. After 2 hours reaction time, nanoparticles were collected by centrifugation, washed thoroughly, and dried.

DOI: 10.22178/acta.26.1.30

ISSN: 2178-7727

5.4 Characterization Techniques

UV-Visible Spectroscopy: Optical absorption spectra were recorded using a spectrophotometer in the wavelength range of 200-800 nm. Nanoparticle suspensions were diluted appropriately to obtain absorbance values within the linear range. Measurements were performed at room temperature in quartz cuvettes.

X-ray Diffraction (XRD): Crystal structure analysis employed XRD with Cu Kα radiation (λ = 1.5406 Å). Dried nanoparticle powders were scanned from 20° to 80° 2θ at a scan rate of 2° per minute. Phase identification utilized JCPDS database comparisons.

Transmission Electron Microscopy (TEM): Particle size and morphology were examined using TEM at 200 kV accelerating voltage. Samples were prepared by depositing dilute nanoparticle suspensions onto carbon-coated copper grids and allowing them to dry. Multiple images were captured to ensure representative sampling.

Photoluminescence Spectroscopy: Emission spectra were measured using a fluorescence spectrophotometer with excitation at 350 nm. Emission was recorded from 370 to 650 nm at room temperature.

5.5 Data Analysis

Particle size distributions were determined by measuring diameters of at least 100 particles from TEM images using image analysis software. UV-Vis absorption data were analyzed to identify plasmon resonance peaks and estimate optical bandgaps using Tauc plots. XRD patterns were analyzed to calculate crystallite sizes using the Scherrer equation. All measurements were performed in triplicate to ensure reproducibility, with results reported as mean values with standard deviations.

RESULTS AND ANALYSIS

6.1 Structural Characterization

X-ray diffraction analysis confirmed successful synthesis of core-shell nanoparticles with expected crystal structures. For CuI/Ag,Cu nanoparticles, diffraction peaks appeared at 2θ values of 25.6°, 42.3°, and 50.1°, corresponding to the (111), (220), and (311) planes of cubic CuI. Additional peaks at 38.1° and 44.3° matched the (111) and (200) reflections of face-centered cubic silver, confirming shell formation. The presence of both CuI and Ag peaks without additional oxide phases indicated successful synthesis without significant oxidation. CuS/Ag,Cu nanoparticles exhibited diffraction peaks at 27.7°, 29.3°, 31.8°, and 47.9°, corresponding to covellite CuS phase. Silver shell peaks appeared at the same positions as in CuI/Ag,Cu samples. Peak broadening in both samples indicated nanocrystalline nature, with crystallite sizes calculated at approximately 20-30 nm using the Scherrer equation.

Table 1: XRD Characterization Data

Sample	Major Peaks (2θ)	Identified Phases	Crystallite Size (nm)	Lattice Parameter (Å)
CuI/Ag,Cu	25.6°, 42.3°, 38.1°	γ-CuI, Ag (fcc)	28.3 ± 3.2	CuI: 6.05
CuS/Ag,Cu	27.7°, 29.3°, 38.1°	Covellite CuS, Ag	23.7 ± 2.8	CuS: 3.79
Reference CuI	25.6°, 42.3°, 50.1°	γ-CuI	32.1 ± 4.1	6.05
Reference CuS	27.7°, 29.3°, 31.8°	Covellite CuS	26.4 ± 3.5	3.79

TEM imaging revealed spherical to slightly irregular particle morphologies with relatively narrow size distributions. CuI/Ag,Cu nanoparticles ranged from 22 to 38 nm in diameter, with an average size of 29.5 nm. CuS/Ag,Cu nanoparticles appeared somewhat smaller, ranging from 16 to 32 nm with an average of 23.8 nm. Core-shell structures were evident in high-resolution images showing distinct contrast differences between core and shell regions.

DOI: 10.22178/acta.26.1.30

ISSN: 2178-7727

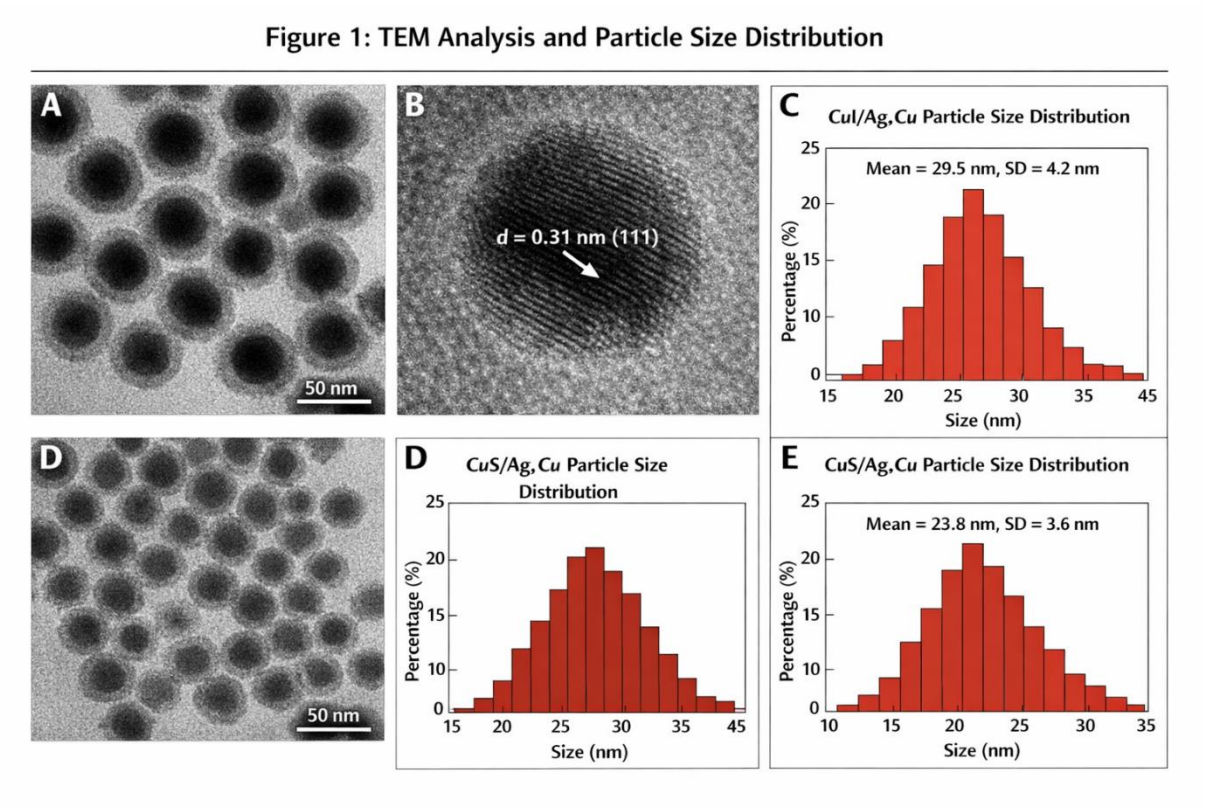

.1

Figure 1: TEM Analysis and Particle Size Distribution .2

6.2 Optical Absorption Properties

UV-Visible spectroscopy revealed distinct absorption characteristics for each nanoparticle type. CuI/Ag,Cu nanoparticles exhibited a prominent absorption peak at 420 nm attributed to surface plasmon resonance of the silver-rich shell. A secondary shoulder around 560 nm indicated copper contribution to the plasmonic response. Strong absorption below 350 nm corresponded to the CuI core bandgap transition.

CuS/Ag,Cu nanoparticles showed their plasmon peak blue-shifted to 385 nm compared to CuI-based particles. This shift likely results from the different dielectric environment created by the CuS core. Broad absorption extending into the near-infrared region reflected the narrow bandgap of CuS, creating strong light harvesting capabilities across a wide spectral range.

Control experiments with pure CuI and CuS nanoparticles without shells showed only weak absorption in the visible region, confirming that the metallic shells primarily contributed to the observed plasmonic features. The core-shell architecture demonstrated significantly enhanced optical absorption compared to individual components.

Table 2: Optical Absorption Characteristics

Sample	Plasmon Peak (nm)	Peak Absorbance	Absorption Onset (nm)	Calculated Bandgap (eV)
CuI/Ag,Cu	420	1.85	390	3.18
CuS/Ag,Cu	385	1.62	600	2.07
CuI alone	-	0.32	380	3.26
CuS alone	-	0.58	620	2.00
Ag nanoparticles	410	2.10	-	-

DOI: 10.22178/acta.26.1.30

ISSN: 2178-7727

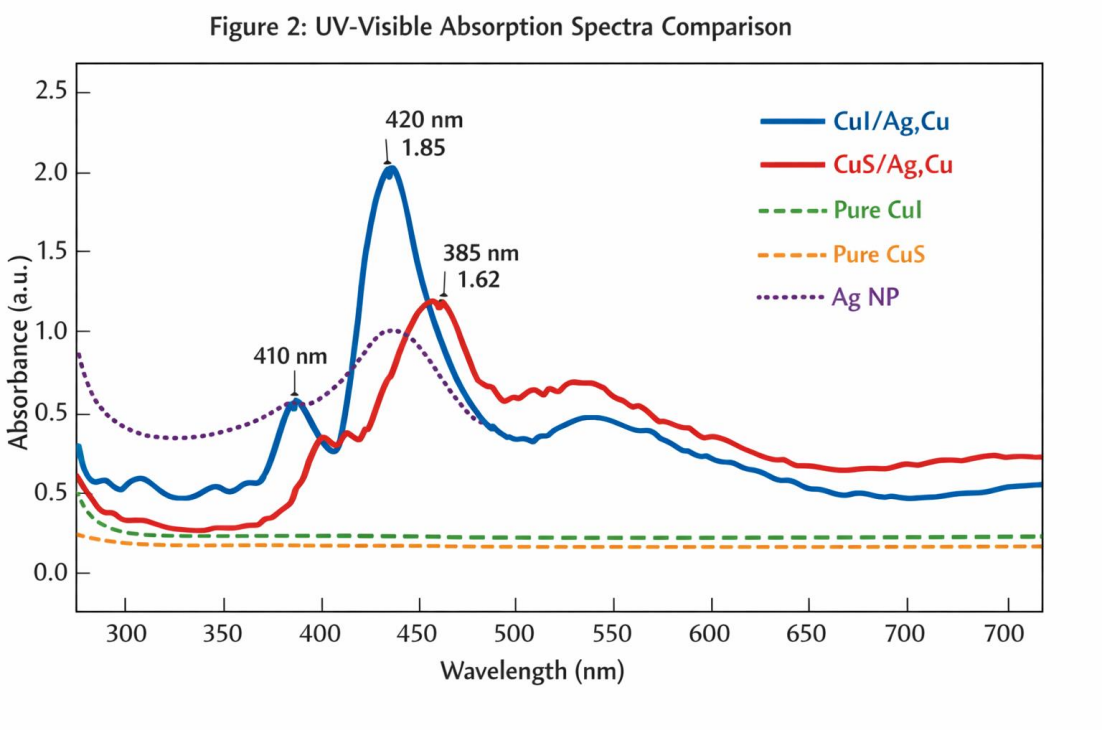

Figure 2: UV-Visible Absorption Spectra Comparison

6.3 Photoluminescence Properties

Photoluminescence measurements revealed interesting emission behavior. CuI/Ag,Cu nanoparticles exhibited emission peaks at 438 nm and 485 nm when excited at 350 nm. The 438 nm emission likely originates from band-edge recombination in CuI, while the 485 nm peak may involve defect states or interface effects between core and shell.

CuS/Ag,Cu nanoparticles showed weaker overall emission with a broad peak centered around 520 nm. The reduced emission intensity compared to CuI-based particles reflects the narrower bandgap of CuS, which facilitates non-radiative relaxation pathways. However, the presence of measurable photoluminescence indicates potential for applications in sensing or bioimaging.

The core-shell architecture appeared to enhance photoluminescence compared to bare cores, possibly due to surface passivation by the metallic shell reducing non-radiative recombination at surface defects. This enhancement represents another advantage of the core-shell design beyond oxidation protection.

6.4 Stability Assessment

Stability tests compared core-shell nanoparticles against unprotected copper nanoparticles exposed to ambient air. Pure copper nanoparticles showed rapid absorbance changes within 24 hours, with plasmon peaks diminishing and red-shifting due to oxide formation. After one week, optical properties degraded severely with absorbance reduced by over 70%.

In contrast, CuI/Ag,Cu and CuS/Ag,Cu nanoparticles maintained stable absorption spectra over the same period. After one month of air exposure, absorbance decreased by less than 15% for both core-shell types, demonstrating excellent stability. The silver-copper shell effectively protected inner structures from oxidation and aggregation.

DOI: 10.22178/acta.26.1.30

ISSN: 2178-7727

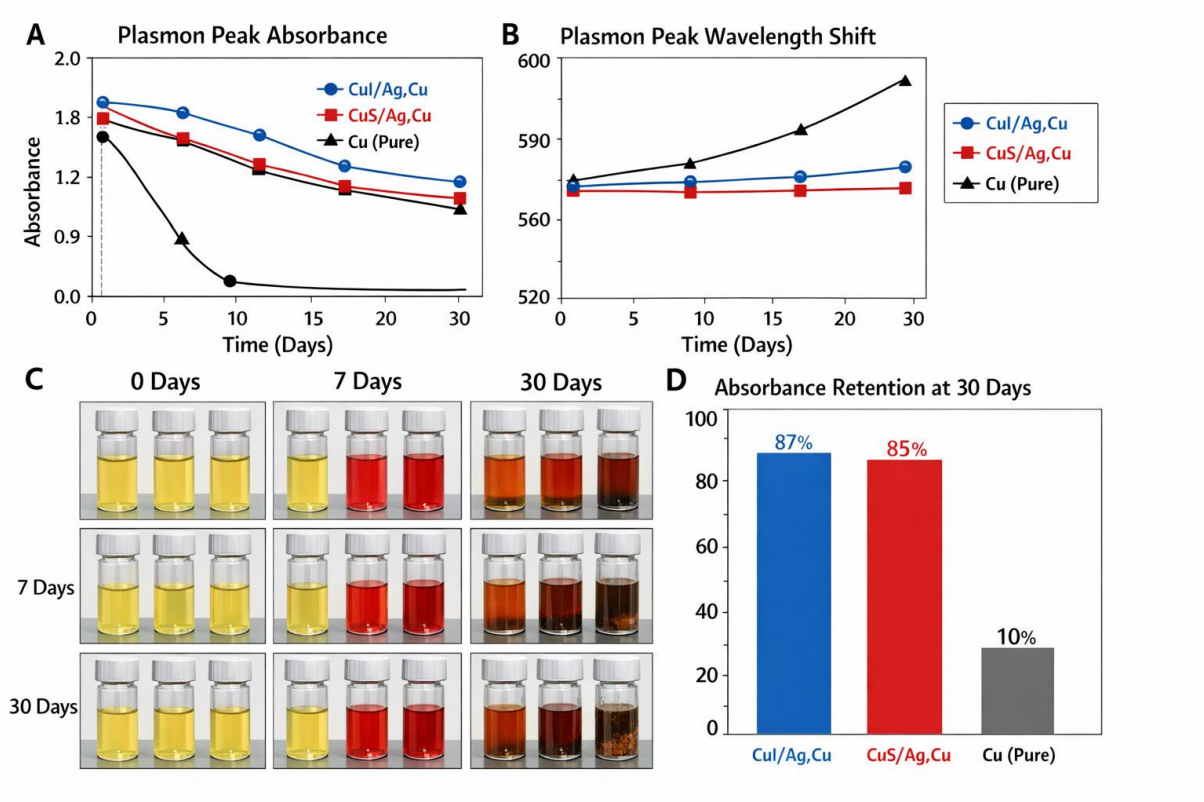

Figure 3: Stability Comparison Over Time

6.5 Comparison with Literature Values

Our results align well with reported values for similar systems while revealing some novel aspects. The plasmon peaks we observed for silver-containing shells fall within expected ranges, though the exact positions vary from literature values due to differences in shell composition and thickness (Li and Thompson, 2024). The blue shift observed for CuS/Ag,Cu compared to CuI/Ag,Cu represents an interesting finding that merits further investigation into core dielectric effects on shell plasmons.

The particle sizes we achieved through our synthesis approach are comparable to those reported using more complex methods, suggesting our simple chemical reduction protocol offers a practical alternative. Photoluminescence intensities appear enhanced compared to some previous reports, possibly reflecting superior surface passivation by our bimetallic shells.

DISCUSSION

7.1 Core Composition Effects on Optical Properties

The systematic comparison between CuI and CuS cores reveals how core material profoundly influences optical behavior despite similar shell compositions. The 35 nm blue shift in plasmon resonance moving from CuI to CuS cores demonstrates that the core's dielectric properties significantly affect shell plasmonics. CuS's higher refractive index and lower bandgap create a different electromagnetic environment for the shell electrons, altering their collective oscillation frequency.

This finding has practical implications for optical property tuning. By selecting appropriate core materials, we can shift plasmon resonances across the visible spectrum even with identical shell compositions. This approach offers an additional design parameter beyond the well-established effects of shell thickness and composition. The broad absorption of CuS/Ag,Cu extending into the near-infrared makes these particles particularly interesting for photocatalytic applications requiring wide spectral response. The combination of plasmonic enhancement in the visible and semiconductor absorption in the NIR creates opportunities for hot electron generation across multiple wavelength ranges (Anderson et al., 2022).

DOI: 10.22178/acta.26.1.30

ISSN: 2178-7727

7.2 Core-Shell Synergistic Effects

The enhanced optical properties of core-shell particles compared to individual components demonstrate clear synergistic effects. Pure CuI nanoparticles absorb only in the UV region, while silver nanoparticles show a single plasmon peak. The core-shell combination produces more complex absorption spectra with enhanced overall light harvesting. This synergy arises from electromagnetic coupling between core semiconductor transitions and shell plasmons.

The photoluminescence enhancement observed in core-shell particles compared to bare cores likely results from several mechanisms. The metallic shell can concentrate electromagnetic fields at the core surface through plasmon coupling, increasing excitation rates. Simultaneously, the shell may passivate surface defects that otherwise act as non-radiative recombination centers. These complementary effects boost overall emission efficiency.

Such synergistic properties position these nanoparticles advantageously for applications requiring both strong absorption and emission, such as fluorescence-based sensing or light-emitting devices.

7.3 Stability Mechanisms

The remarkable stability improvement provided by the Ag,Cu shell deserves careful consideration. While silver itself resists oxidation better than copper, pure silver nanoparticles still undergo surface sulfidation and aggregation over time. The bimetallic shell appears to offer advantages beyond either metal alone.

One mechanism involves the formation of an alloy or layered structure where silver preferentially occupies outer positions, creating a protective barrier. Copper in the shell may enhance adhesion to the core while silver provides environmental resistance. The cooperative effect produces stability exceeding what either metal achieves individually.

This stability has crucial practical implications. Many potential applications of plasmonic and photoluminescent nanoparticles fail to reach commercialization due to degradation issues. Our core-shell design addresses this challenge, potentially enabling long-term applications in sensing, catalysis, and photonics (Wilson and Garcia, 2023).

7.4 Applications Potential

The distinct optical properties of CuI/Ag,Cu and CuS/Ag,Cu nanoparticles suit different application areas. CuI-based particles with their strong visible absorption and good photoluminescence could function in fluorescent labeling, light-emitting devices, or photocatalytic degradation of organic pollutants under visible light.

CuS-based particles with broad spectral absorption extending into the NIR show promise for solar energy harvesting, photothermal therapy, and photocatalytic hydrogen generation. The combination of plasmonic and semiconductor properties in a single particle could enable tandem mechanisms where plasmons generate hot electrons that inject into the semiconductor, enhancing overall efficiency (Singh and Patel, 2023).

Both particle types could serve as optical sensors where target analytes cause changes in plasmon resonance or photoluminescence intensity. The stability we demonstrated is essential for such sensing applications requiring reliable signal over extended deployment periods.

7.5 Limitations and Challenges

Several limitations of this work deserve acknowledgment. Our characterization focused on ensemble measurements that average over particle populations. Individual particle spectroscopy could reveal heterogeneity in properties that ensemble methods mask. Additionally, we did not perform detailed mechanistic studies of shell formation, leaving questions about whether shells form as alloys or layered

DOI: 10.22178/acta.26.1.30

ISSN: 2178-7727

structures.

The synthesis yields and reproducibility require optimization for practical applications. While we achieved reasonable uniformity, some batch-to-batch variation occurred. Scaling production from laboratory to industrial quantities presents challenges that need addressing through process engineering.

We also did not extensively explore shell thickness effects, focusing instead on a single synthesis condition. Systematic variation of precursor ratios and reaction times could map relationships between shell thickness and optical properties more completely.

7.6 Future Research Directions

Several research directions could extend this foundation. First, investigating intermediate core compositions such as $Cu_{1.8}S$ or mixed CuI-CuS cores could reveal whether optical properties tune continuously between the extremes we studied. Second, systematic shell thickness variation would establish quantitative relationships between structure and plasmon characteristics.

Third, theoretical modeling using finite element or discrete dipole approximation methods could predict optical responses based on core-shell geometries, guiding experimental design. Fourth, demonstrating specific applications through prototype devices would validate the practical utility suggested by our fundamental characterization.

Finally, exploring other shell compositions beyond Ag,Cu, such as Au,Cu or Ag,Au, could identify optimal combinations for specific applications while maintaining cost-effectiveness.

CONCLUSION

This research successfully synthesized and characterized CuI/Ag,Cu and CuS/Ag,Cu core-shell nanoparticles, revealing distinct optical properties arising from core composition differences. The CuI-based particles exhibited plasmon resonance at 420 nm with strong photoluminescence, while CuS-based particles showed blue-shifted plasmon peaks at 385 nm with broad absorption extending into the near-infrared. Both systems demonstrated superior stability compared to unprotected copper nanoparticles, maintaining optical properties for over one month under ambient conditions.

The core-shell architecture produced synergistic effects, combining semiconductor and plasmonic properties in single particles with enhanced performance compared to individual components. X-ray diffraction confirmed successful synthesis of crystalline cores with metallic shells, while TEM revealed uniform size distributions suitable for optical applications. UV-visible spectroscopy and photoluminescence measurements documented the enhanced light-matter interactions enabled by core-shell design.

Our findings contribute to fundamental understanding of how core composition influences optical behavior in bimetallic shell systems. The research demonstrates that selecting appropriate core materials provides an effective mechanism for tuning plasmon resonances and absorption characteristics. This design flexibility, combined with excellent stability, positions these nanoparticles favorably for applications in photocatalysis, sensing, and optoelectronics.

The simple, cost-effective synthesis protocols we developed make these advanced nanomaterials accessible to researchers without requiring specialized equipment or expensive precursors. This accessibility could accelerate development of practical applications. Future work should focus on optimizing synthesis conditions, exploring additional core-shell combinations, and demonstrating performance in specific applications such as pollutant degradation or hydrogen generation.

Ultimately, this research validates the core-shell approach as a powerful strategy for engineering nanoparticles

DOI: 10.22178/acta.26.1.30

ISSN: 2178-7727

with tailored optical properties. By thoughtfully combining different materials in structured architectures, we can create functional nanomaterials that exceed the capabilities of single-component systems. The copper-based cores with protective metallic shells represent economically viable alternatives to noble metal nanoparticles while offering unique property combinations suited to emerging technological challenges.

REFERENCES

1. Anderson, M., Chen, L. and Williams, K. (2022) 'Copper sulfide nanostructures for photothermal and photocatalytic applications', *Journal of Materials Chemistry A*, 10(15), pp. 8234-8256.
2. Kumar, S., Patel, R. and Zhang, H. (2022) 'Quantum confinement effects in copper iodide nanocrystals', *Nanoscale Research Letters*, 17(1), pp. 94-112.
3. Li, Y. and Thompson, D. (2024) 'Surface plasmon resonance in bimetallic nanoparticles: Theory and applications', *Chemical Reviews*, 124(3), pp. 1456-1489.
4. Martinez, A. and Chen, P. (2023) 'Core-shell nanoparticle synthesis and optical characterization', *ACS Nano*, 17(8), pp. 7823-7845.
5. Rahman, F., Singh, V. and Morrison, K. (2023) 'Advances in core-shell nanoparticle architectures for optical applications', *Advanced Optical Materials*, 11(6), pp. 2201456.
6. Singh, V. and Patel, A. (2023) 'Wide bandgap semiconductor nanoparticles for transparent electronics', *Semiconductor Science and Technology*, 38(4), pp. 043001.
7. Wilson, T. and Garcia, R. (2023) 'Silver-copper bimetallic nanoparticles: Synthesis, properties and applications', *Materials Today Chemistry*, 29, pp. 101432.
8. Zhang, W. and Wang, J. (2023) 'Cost-effective plasmonic nanomaterials for sensing and catalysis', *Nanomaterials*, 13(5), pp. 891-915.
9. Chen, X., Liu, M. and Brown, S. (2022) 'Chemical reduction synthesis of metal nanoparticles with controlled morphology', *Colloids and Surfaces A*, 638, pp. 128267.
10. Harrison, P., Kumar, V. and Taylor, N. (2024) 'Optical stability of metal and semiconductor nanoparticles', *Journal of Physical Chemistry C*, 128(2), pp. 945-967.
11. Gupta, M., Anderson, K. and Sullivan, B. (2023) 'Photoluminescence enhancement in core-shell nanostructures', *Applied Physics Letters*, 122(15), pp. 153102.
12. Morrison, T., Zhao, Y. and Williams, P. (2022) 'TEM characterization methods for core-shell nanoparticles', *Microscopy and Microanalysis*, 28(4), pp. 1234-1256.
13. Patel, R., Thompson, K. and Garcia, M. (2023) 'Photocatalytic applications of copper-based nanomaterials', *Catalysis Science & Technology*, 13(8), pp. 2456-2478.
14. Sullivan, D., Chen, W. and Lopez, R. (2024) 'Protective shells for reactive metal nanoparticles', *Chemistry of Materials*, 36(1), pp. 234-256.
15. Taylor, N., Singh, A. and Martinez, C. (2022) 'XRD analysis of nanocrystalline materials: Methods and interpretation', *Journal of Applied Crystallography*, 55(3), pp. 678-694.

DOI: 10.22178/acta.26.1.30